EasyChair Preprint

№ 9028

Evaluating the Mechanical Properties of Isolated Rat Cardiomyocytes Sarcolemma Using Atomic Force Microscopy

Ahmad A. Almazloum, Monica Alonso Cotta,
José Wilson Magalhaes Bassani and Rosana Almada Bassani

October 8, 2022

Evaluating the Mechanical Properties of Isolated Rat Cardiomyocytes Sarcolemma Using Atomic Force Microscopy

A.A. Almazloum[1], M.A. Cotta[2] J.W.M Bassani[1,3] and R.A. Bassani[1,3]

[1]Department of Electronics and Biomedical Engineering, School of Electrical and Computer Engineering; University of Campinas (UNICAMP), Campinas, SP, Brazil
[2] Department of Applied Physics, Institute of Physics "Gleb Wataghin", UNICAMP, SP Brazil
[3]LabNECC, Center for Biomedical Engineering, UNICAMP, Campinas, SP, Brazil

Abstract— Incidence of cardiac diseases, one of the leading causes of death worldwide, is still on the rise. As the cardiomyocyte is the contractile unit of the heart, knowledge on the details of its mechanical structure and functionality is helpful to the understanding of myocardial pathophysiology and development of therapeutic approaches. Atomic force microscopy (AFM) has been used not only for topographic surface imaging but also for direct assessment of the mechanical characteristics of the plasma membrane. In this work, a preliminary study was conducted focusing on factors affecting the elasticity (***E***) of the sarcolemma (SL) of isolated rat ventricular myocytes, which was determined using AFM. After collecting the topographic image, 16×16 force map was generated and post-analyzed curve by curve using the Hertz model to estimate the Young's modulus (i.e., ***E***). The influence on ***E*** was investigated for the factors: position (32), cell (18), heart (12), and post-isolation storage period. Appreciable variability was observed for all factors. Considering all studied cells, the mean ***E*** value was lower than reported in the literature (~11 vs. 35-40 kPa). This might be attributed to different maximum forces, speeds and depths of indentation which could have a great influence on ***E***. Also, longer storage was associated with decreased ***E*** values (<10h: 10.96±0.08kPa; n=5902; >12h; 6.48±0.05kPa; n=2012), probably due to cell deterioration with time. Accurate measurement of ***E*** is essential to detect alterations in cell function and effect of therapeutic drugs due to changes in SL mechanical properties. From the present results, it is possible to conclude that storage must be as short as possible, and that other alternatives should be sought for verifying cell viability and improving cell attachment.

Keywords— **Cell mechanics; cardiomyocyte; sarcolemma; elasticity; force spectroscopy.**

I. Introduction

Elasticity, viscoelasticity or stiffness are frequently used to evaluate the mechanical properties of the plasma membrane (sarcolemma, SL, in myocytes) of living cells, which greatly impacts cell function. Elasticity (represented by the Young's modulus, ***E***) is an intensive property of solid materials that describes the relationship between the mechanical stress (force) and the strain (deformation) [1]. Deviation of plasma membrane ***E*** values from the normal range may indicate defects (e.g., pathologies), and ***E*** determination may help assessing the effect of treatments, such as drugs, in living cells/tissues [2]. Many techniques have been used to estimate ***E*** of living materials, such as optical tweezers, micropipette aspiration, tracing force microscopy, and atomic force microscopy (AFM) [1, 2]. The latter offers high resolution of surface topography and interaction force in the sub-nanometer and pico-Newton ranges, respectively, which is appropriate for biological samples, especially myocytes [1, 2, 3, 4].

AFM is commonly used for force spectroscopy, in which an external vertical force is applied to the sample via the tip, with a well-defined geometry and spring constant, mounted on a cantilever [1]. AFM has been used on several cell types to produce SL surface topography and force maps. To obtain high resolution topographic images, fixation (e.g., with glutaraldehyde) has been used to assure cell immobility. On the other hand, this chemical treatment has adverse effects on cell viability and may modify membrane mechanical properties [1, 2], thus compromising the reliability of ***E*** estimation.

Investigation of the mechanical properties of ventricular myocytes is relevant, considering that alterations in membrane elasticity may be accompanied by cell dysfunction. By allowing the generation of force maps, force spectroscopy has been used to determine SL ***E*** in several cell types, but very few studies were performed on cardiomyocytes, investigating alterations in SL ***E***, associated with aging and diabetes [3, 4].

In this study, we present some preliminary results and considerations on the estimation of ***E*** for (presumably) live isolated rat cardiomyocytes in a physiological liquid environment, following different periods of post-isolation storage in cardioplegic solution. Considering factors that may affect the reliability of the results, variability of the measurements was evaluated at different levels: among scanned positions in the same cell, among myocytes of the same heart, among hearts, and in fresh versus stored myocytes.

II. MATERIAL AND METHODS

A. Isolated cardiomyocytes

Protocols of animal care and use were approved by the institutional Committee of Ethics in Animal Use (CEUA/IB/UNICAMP; process number 4429-1/2019). Myocytes were isolated from the left ventricle of adult (3-5-month-old) male Wistar rats (n= 12) by enzymatic digestion with collagenase I via coronary perfusion, as previously described by Penna and Bassani [5]. After digestion, the left ventricle was dissected and cells were mechanically dissociated in cardioplegic solution, with the following composition (in mM): 30 KCl, 10 KH_2PO_4, 1 $MgCl_2.6H_2O$, 10 N-2 hydroxyethylpiperazine-N"-2 ethane-sulfonic acid (HEPES), 11 glucose, 20 taurine, 70 glutamic acid, 1 mg/ml bovine serum albumin, pH 7.4

Myocytes were kept in the cardioplegic solution at 4 °C until use. Before use, cells were left to sediment by gravity and the pellet was washed 2-3 times with Ca^{2+}-free Tyrode´s solution (composition in mM: 140 NaCl, 6 KCl, 2.5 MgCl2, 10 HEPES, 11 glucose; pH 7.4) to remove the cardioplegic solution and debris. The cell suspension in the Ca^{2+}-free Tyrode's solution was added to the AFM liquid cell (chamber), of which the coverslip bottom was treated with collagen to facilitate cell adhesion. Ca^{2+} was removed from the extracellular medium to minimize spontaneous contractions, which is crucial to decrease noise of the force map recordings and to prevent the myocyte from adhering to the cantilever tip. It is noteworthy that ***E*** of myocyte SL does not appear to be affected by major decreases in extracellular Ca^{2+} concentration [4].

B. Atomic Force Microscopy System

Surface topography and force curve maps were produced with a 5500 Scanning Probe Microscope (Keysight, Technologies, USA) which has a video camera system to align the laser on the cantilever. This provides good-quality optical images of the samples.

A soft silicon nitride probe MSCT (Bruker AFM Probes, CA, USA) was used. This probe has a triangular *cantilever A* (L= 175 µm, W= 22 µm, spring constant (*k*)= 0.07 N/m, resonance frequency (f_0) = 22 kHz), with a pyramidal tip with 20 ± 1.25° half-opening angle, 5 µm height and 10 nm radius at the extremity. However, because the nominal specifications of the cantilever have a wide range of tolerance, we used the thermal noise method (thermal tuning) [6], implemented in this microscope, to determine f_0 and *k* experimentally. The fact that both f_0 and *k* have a large variability comes from the uncertainty on the cantilever dimensions, particularly its thickness [7, 8]. That is why *k* calibration needs to be repeated each time that the probe is installed or even markedly drifts from its position during the measurements [7, 8].

The values of mean ± standard error of the mean (SEM) of f_0 and *k* obtained with the thermal noise method were, respectively, 23.3 ± 1.6 kHz and 0.051 ± 0.006 N/m (n= 12). The deflection sensitivity (*def*), which is another calibration for the laser system that includes the optical detectors, showed a larger variability (1.75 ± 0.16 µm/V; n= 12). This is due to *def* dependence on the system alignment: the laser incidence on the cantilever, its reflection received by the detector and even the transmission medium. Thus, the presence of particles in suspension in the solution may affect the *def* value. The calibration of *def* was carried out according to standardized protocols in the literature [7, 8], in a clean liquid cell containing the Ca^{2+}-free Tyrode's solution, but not cells, and considering the chamber bottom as an infinite rigid surface.

C. Experimental Protocol

Experiments were carried out at 25 ± 3 °C. After spreading collagen solution on the coverslip bottom of the liquid chamber, it was allowed to dry for 15 min. Then 500 µL of the myocyte suspension in Ca^{2+}-free Tyrode's solution were pipetted in the liquid cell, and cells were left to settle down and adhere to the chamber bottom for 30 min. Care was taken not to extend this sedimentation period because all measurements needed to be made within 1 hour after the sample insertion in the AFM head, after which the preparation was discarded. Even though the cardiomyocyte oxygen consumption is lower in Ca^{2+}-free Tyrode, cells tend to deteriorate after a long time without perfusion, which introduces more variability to the measurements [2]. Cells were used between 1-10 (**fresh group**) and 12-24 h (**stored group**) after isolation.

After choosing a rod-shaped, striated myocyte with fairly straight borders and not in contact with other cells, the tip of the cantilever was moved upon the cell surface to produce a surface topographic image in the contact mode. Three transversal regions were delimited along the whole major axis of the cell. Avoiding the central region, which usually contains the nucleus, the tip of the cantilever was positioned upon either of the two remaining regions (extremities). The topographic image covered a 20×20 μm^2 area and the scanning speed varied between 0.3-1.0 lines/s according to the surface topography. The SL was scanned by applying a force of 0.86 ± 0.15 nN (n= 32), sufficient to track the myocyte surface. Then, a 16×16-matrix of force curves, known as force-volume map, was obtained after generating a good-quality topographic image and also some individual force curves to calibrate the ramp range. This ramp (i.e., the distance travelled by the cantilever in the approach and retraction phases, to generate the force curve), depended on the height variation measured in the topographic image. Because this variation

was on the average 3.85 µm, the indentation speed was set as low as 2 µm/s with wide ramp to increase the possibility to find the contact point correctly. A limit of 5 nN was preselected as a precaution to avoid SL damage or getting the cell stuck on the tip, which might have required recalibrating or even exchanging the cantilever.

Empirically, the suitable force to be applied could be established as the minimum force necessary to produce a standard force curve (see Fig. 1), taking into consideration an adequate indentation distance. Indentations were limited to a maximum of 1.5 µm (~10 % of the average myocyte height [10, 13]) and a minimum of 0.5 µm (necessary for an acceptable precision in the detection of the contact point in the force curve [9, 11]). It is important to mention that adhesion forces and hysteresis were kept to a minimum by reducing the approach/retraction velocity (2 µm/s in this study), which minimizes energy dissipation [2, 3] and thus allows a more precise $\boldsymbol{E}$ estimation,

After obtaining a 256 force curve maps for the first position, a different position (preferentially in other cell positions) was selected and the whole procedure was repeated. In some cases, it was not possible to obtain more than a couple of maps because of myocyte instability (lack of adequate adhesion to the chamber bottom) or lack of time, due to the limited cell viability interval for measurement acquisition. The absence of cell damage or morphological alteration during the measurement procedure was carefully monitored by the optical image to assure data reproducibility.

D. Data Analysis

All topographic images, force curves and maps were analysed with *AtomicJ* [12] and *Gwyddion* [13] programs, which are free software. Firstly, the topographic images were pre-processed to improve contrast. Artifacts and surface flatness were corrected by aligning the rows using the polynomial method (degree 3) after removing the background (degree 2). Subsequently, mean and root mean square (RMS) roughness values were calculated for a 10×10 µm^2 central mask to reduce the effect of the scanner curvature (range = 90 µm). Then, a 3-dimensional projection was generated to allow a better representation of the surface topography. Secondly, force curves were pre-processed by applying a 2nd-degree Gaussian filter to remove noise and improve detection of the contact point [9, 11]. In this step, curves were verified individually for adherence to the standard configuration, otherwise they were discarded.

As shown in Fig. 2, the standard force curve has two phases: approach (magenta) and retraction (green). The former starts with a horizonal baseline (at least 0.5 µm) followed by a continuous ascending line with slope< 1 (vertical) reaching the setpoint (transition) without abrupt peaks or valleys. The retraction phase has the same form in the reversed order, but it has a valley at the end of the descending line before the baseline, caused by the adhesion of the sample to the tip.

The Hertz model for pyramidal tips modified by Sneddon [14] and later by Bilodeau [15] was selected to fit the approach curve. Following the procedure of automatic detection of the contact point [12], each individual force curve in each force map was checked for successful determination of the contact point. The criterium of contact point detection depended simply on the *equation 1* of the model, which represents the points of an ideal curve resulting from exerting on the sample a vertical force F by an indenter with pyramidal geometry:

$$F = \frac{E^* \tan\theta}{\sqrt{2}}\delta^2 \qquad (1)$$

where E^* is the reduced Young's modulus of the tip material, θ is the half-opening angle of the pyramid and δ is the indentation into the sample. For tips made of materials much stiffer than the sample, $E^* \cong E/(1-\nu^2)$, where E is the Young's modulus and ν is the Poisson ratio of the sample ($\nu = 0.5$ for incompressible materials, such as the cytoplasm).

Knowing that the cantilever can be considered as a linear spring, Hook's law can be applied (*equation 2*):

$$F = k.(d - d_0) \qquad (2)$$

where k is the spring constant expressed as N/m and $\Delta d = (d - d_0)$, i.e., the cantilever deflection starting from the contact point (z_0, d_0), which should be converted from V into nm by multiplying it by *def* [nm/V]. For the special case of very rigid materials, the displacement on the vertical axis equals the deflection of the cantilever, but for soft materials, this equality is not valid and indentation in the sample can be described by the *equation 3*, assuming that z is the movement of the piezo-electric motor:

$$\delta = (z - z_0) - (d - d_0) \qquad (3)$$

Thus, combining *equations 1, 2* and *3*, Δd can be calculated as [16]:

$$z - z_0 = (d - d_0) + \sqrt{\left(\sqrt{2}.\frac{k(d - d_0)(1-\nu^2)}{E\tan\theta}\right)} \qquad (4)$$

With k and d_0 obtained from the calibrations and the baseline, *equation 4* was used to fit the approach curve, from which E and z_0 were retrieved. By comparing the experimentally determined curves with the model, it was possible to select for further analysis only the curves with coefficient of determination (R^2) value ≥ 0.95.

Histograms, box-and-whisker plots and maps were generated for each individual scanned position and pooling all positions. Depending on the histogram distribution, the mean (normal distribution) or the median (Lorentz distribution) was considered for $\boldsymbol{E}$. Additionally, 2D $\boldsymbol{E}$ maps were produced, in which each pixel represents the stable $\boldsymbol{E}$ value (20×20 µm^2

contact image with 256 pixels). Other maps, such as of contact point, deformation and adhesion force, were also generated and checked for anomalies.

Data are presented as means ± SEM.

III. Results and Discussions

A. Images of Surface Topography

Tridimensional topographical surface images using the contact mode were obtained from 18 cells in at least one position. The surface topography was characterized by quantitative analysis. Fig. 1 illustrates the surface topography of a myocyte within a 20×20 µm² area, in which micro-irregularities can be detected within 0.7 µm.

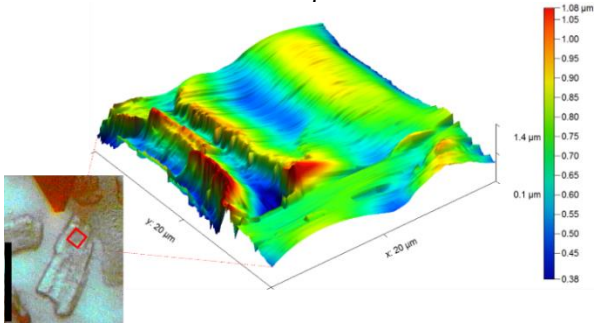

Fig. 1: Tridimensional surface topology of the sarcolemma of a rat ventricular myocyte, generated from AFM contact image, showing micro-irregularities up to 0.7 µm depth, where tips and valleys were colored in red and blue, respectively. Inset: optical microscopic image of the cell, where the red square indicates the region from which the force map was obtained and the black vertical bar measures 100 µm.

As expected, the RMS roughness was greatly reduced by preprocessing and artifact correction, from 823.34 ± 62 to 34.53 ± 8 nm (n= 32). Interestingly, fresh myocytes had greater roughness than stored ones (41.0 ± 10.0 nm; n= 24, vs. 14.4 ± 17.0 nm; n= 8 (p= 0.010; *t* test for heteroscedastic variances).

B. Image Force Mapping:

Of the 8064 force curves obtained from 32 positions in 18 different myocytes isolated from 12 hearts, 98% were considered suitable for further analysis, according to the criteria previously described. Fig. 2 shows examples of force-distance, force-indentation and ***E***-indentation curves, and Fig. 3 shows the frequency-histogram of ***E*** values obtained from a single position with 16×16 force curves.

After analyzing each individual force map (scanned position) for all cells obtained from all hearts, a global histogram and box-and-whisker plot were created. The former offers an overall view of all force curves and enables fitting the data distribution, while individual box-and-whisker plots allows comparing multiple sources of variations: position (in the same cell), cells (from the same heart), and hearts.

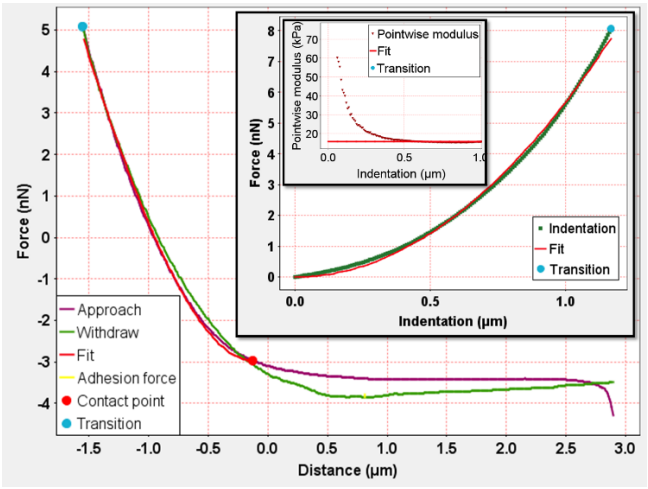

Fig. 2: Force-distance curve obtained by AFM spectroscopy in a cardiomyocyte, taken from a 16×16 force map after the generation of a 20×20 µm² contact topographic image. The main graph shows the approach (magenta) and withdraw (green) phases and the fitted curve (red). Inset: proportion of the applied force within the indented distance, starting from the contact point. Inset in the inset: pointwise calculation of the Young's modulus (***E***) for each individual point in the indentation trace, stability of the ***E*** value when indentation > 0.5 µm. The maximum indenting force in this curve was ≈ 5 nN.

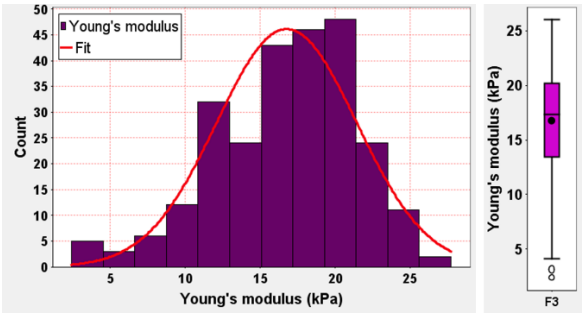

Fig. 3: Left: frequency histogram of the Young´s module in cardiomyocytes, fitted with a normal distribution curve (red) (16.77 ± 0.29 kPa; n= 256). Right: box-and-whisker plot showing mean and median (central dot and line, respectively) and interquartile interval (box) of the Young's modulus obtained with AFM spectroscopy force mapping (16x16 maps) in a single fresh myocyte. The whiskers indicate the minimum e maximum values. Outliers are shown when their values exceed 1.5 times that of the interquartile range above (none here) or below the limits of the latter.

Fig. 4 illustrates a global histogram, fitted with the Lorentz distribution fit (in red) (***E***= 10.96 ± 0.08 kPa; n= 5902). Two peaks can be distinguished in the histogram, at ~4 kPa and ~13 kPa, which can possibly be attributable to scanning over the cell nucleus, as this organelle was not always centrally located, compared with other peripheral regions [17].

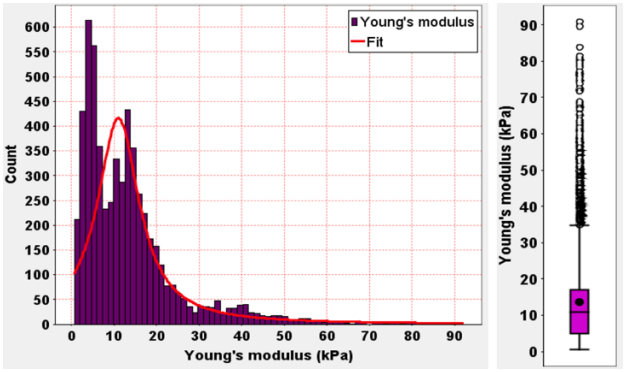

Fig. 4. Similar presentation as in Fig. 3, but with data from a larger sample (fresh group: 5904 force curves, 24 positions, 13 cells, 9 hearts). The curve fitted for Lorentz distribution of the histogram is shown in red (10.96 ± 0.08 kPa) and the respective box-and-whisker plot (right) for Young's modulus. For description of the box-and-whisker plot see the caption in Fig. 3

C. Impact of the Scanned Region on SL Elasticity

Fig. 5 shows differences in the ***E*** values among 3 indented positions in the same myocyte, such as F6-1, F6-2 and F6-3; F4-1 and F4-2; F8-1 and F8-2, and F10-1 and F10-2, although not in all cells. This variation, also seen in other cell types, might be explained to non-homogeneous spatial distribution of subsarcolemmal structures, such as cytoskeleton and cytoplasm [18]. As in skeletal myocytes, the SL of ventricular myocytes present a periodic structure characterized by invaginations (T tubules) at the line Z, where ***E*** is greater [19].

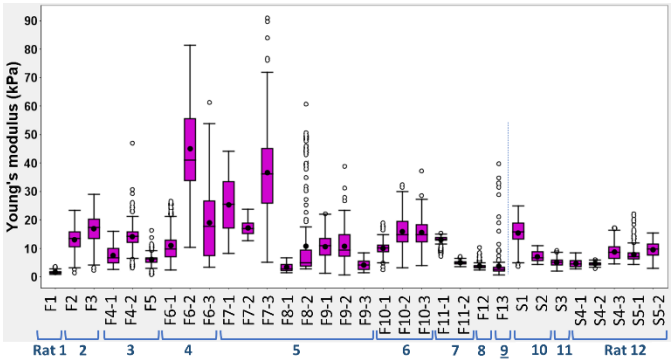

Fig. 5: Box-and-whisker plots of the sarcolemmal elasticity (Young's modulus) estimated by AFM spectroscopy force mapping in rat cardiomyocytes at different scanning positions (16×16 force maps: 7914 force curves, 32 positions, 18 cells, 12 hearts). Data are shown as described in the caption of Fig. 3, for cells from the fresh (F) and stored (S) groups (see Material and Methods). The 1st algorism after the group code is the cell number, and the 2nd, when present, indicates different scanned positions. "Rat" (bottom) indicates the heart from which myocytes were isolated. The boxes are computed from 209 curves at least (max= 256), except for cell F1, for which only 93 curves were used.

D. SL Elasticity: Inter-cell and Inter-heart Variability and Impact of the Time of Storage

As shown in Fig. 6, ***E*** varied between 3 and 40 kPa among cells. This large variability might be attributed to different degrees of SL integrity. Intact, freshly isolated myocytes have firmer and tenser structure than the older cells. Accordingly, ***E*** values in the fresh group were generally higher than in the stored group (***E***= 10.96 ± 0.08 kPa; n= 5902 vs. 6.48 ± 0.05 kPa; n= 2012, respectively). Decrease in SL ***E*** was reported in fibroblasts under cytotoxic conditions that lead to cytoskeletal disruption [20]. Also, cell death associated with SL permeabilization (verified by intracellular staining with propidium iodine) is accompanied by a fall in ***E*** values [21].

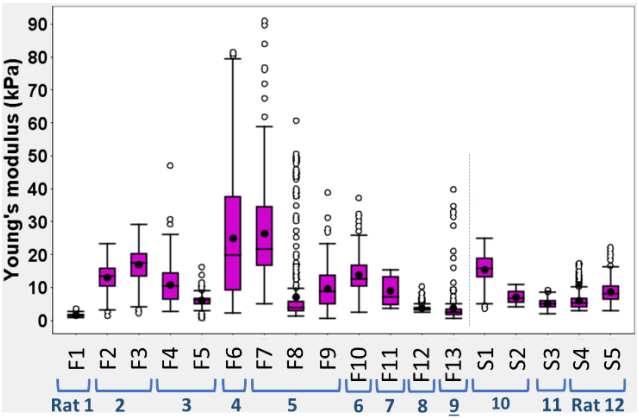

Fig. 6: Young's modulus of cardiomyocytes sarcolemma estimated by AFM spectroscopy force mapping. Data are the same as in Fig, 6, except those points of different scanned positions of the same cell were pooled.

Approach/withdraw speed and maximum indenting force were found to have substantial impact on ***E*** values. An indentation velocity of 0.6-6 µm/s is suitable to reduce hysteresis [3,4], so 2 µm/s was used in this work. Another probable source of variability might be the presence of molecules anchored to the external SL face [7, 22]. The geometry of the indenting tip is another important factor to determine the detected features of the SL surface. Sharp tips, as used in this study, usually result in ***E*** overestimation when under high applied forces, compared with blunted, truncated or colloidal ones. However, previous studies with rodent cardiomyocytes [3, 4] reported higher mean ***E*** values than in the present report (~35-40 vs. ~11 kPa), although we have obtained values > 20 kPa in a number of cases.

The present results indicate that methodological improvement is necessary. For instance, cell viability was confirmed simply by myocyte appearance, a method which is not the most adequate. Working with freshly isolated myocytes rather than cultured cells requires efficient means of cell immobilization. Adhesion to the collagen layer is not sufficiently

strong and not spatially homogeneous, and a more suitable substrate should be used. Finally, cell storage for several hours should be avoided. Understanding how these problems may affect the collected data is important to set the limitations necessary for elaborating the experimental protocols for this kind of experiment with cardiomyocytes.

IV. Conclusions

Several factors such as scanned position, indentation speed, maximum indenting force, indentation depth, tip's shape of the probe, and storage time for cells may influence ***E*** determination, taking into consideration the heterogeneous structure of this cellular type. These preliminary experiments performed under challenging conditions (i.e., loosely attached contractile cells with high degree of SL corrugation [10], absence of extracellular Ca^{2+}) are helpful to reveal crucial methodological aspects that are important for reliable measurements and result interpretation.

Acknowledgment

The technical support of Ms. Elizângela S. Oliveira and Mr. João H. Clerici is greatly appreciated. Financial support: Brazilian National Council for Scientific and Technological Development (CNPq, Proc. N. 304010/2016-2 and 429326/2018-1), São Paulo Research Foundation (FAPESP 2019/07616-3), Brazilian Ministry of Health/FINEP (grant# 01-13-0214-00) and Coordination for the Improvement of Higher Education Personnel (CAPES, Ph.D. scholarship for A.A. Almazloum).

Conflict of interest

The authors declare that they have no conflict of interest.

References

1. Moeendarbary E, Harris AR. (2014) Cell mechanics: principles, practices, and prospects. WIREs Syst Biol Med 2014, 6:371–388.
2. Lachaize V, Formosa-Dague C, Smolyakov G et al. (2015) Atomic force microscopy: an innovative technology to explore cardiomyocyte cell surface in cardiac physio/pathophysiology. Lett Appl NanoBioSci, 4:321-324.
3. Lieber SC, Aubry N, Vatner SF et. al. (2004) Aging increases stiffness of cardiac myocytes measured by atomic force microscopy nanoindentation. Am J Physiol Heart Circ Physiol 287:H645–H651. DOI: 10.1152/ajpheart.00564.2003
4. Benech JC, Benech N, Damián JP et. al. (2013) Diabetes increases stiffness of live cardiomyocytes measured by atomic force microscopy nanoindentation. Am J Physiol Cell Physiol 307:C910–C919. DOI: 10.1152/ajpcell.00192.2013
5. Penna LB, Bassani RA. (2010) Increased spontaneous activity and reduced inotropic response to catecholamines in ventricular myocytes from footshock-stressed rats. Stress 13:73-82.
6. Butt H-J, Jaschke M. (1995) Calculation of thermal noise in atomic force microscopy. Nanotechnology 6:1.
7. Schillers H. (2019) Measuring the elastic properties of living cells. In: Santos N., Carvalho F. (eds) Atomic Force Microscopy. Methods in Molecular Biology, vol 1886. Humana Press, New York.
8. Schillers H, Rianna C, Radmacher M et. al. (2017) Standardized nanomechanical atomic force microscopy procedure (SNAP) for measuring soft and biological samples. Sci. Rep. 7, 5117.
9. Gavara N, Chadwick RS. (2012) Determination of the elastic moduli of thin samples and adherent cells using conical atomic force microscope tips. Nature Nanotech 7:733–736.
10. Milan HFM, Bassani RA, Santos LEC et. al. (2019) Accuracy of electromagnetic models to estimate cardiomyocyte membrane polarization. Med Biol Eng Comput 57:2617–2627.
11. Rico F, Roca-Cusachs P, Navajas D et. al. (2005) Probing mechanical properties of living cells by atomic force microscopy with blunted pyramidal cantilever tips. Phys. Rev. E 72, 021914.
12. Hermanowicz P, Sama M, Gabrys H et al. (2014) AtomicJ: an open source software for analysis of force curves. Rev. Sci. Instrum. 85, 063703 DOI: 10.1063/1.4881683
13. Nečas D, Klapetek P (2012). Gwyddion: an open-source software for SPM data analysis. Cent. Eur. J. Phys., 10:181-188
14. Sneddon IN. (1965) The relation between load and penetration in the axisymmetric boussinesq problem for a punch of arbitrary profile. Int J Engin Sci 3:47-57.
15. Bilodeau GG. (1992) Regular pyramid punch problem. J Appl Mech, 59:519-523.
16. Radmacher M. (2002) Measuring the elastic properties of living cells by AFM. In: Methods in Cell Biology: Atomic Force Microscopy, ed. by Jena BP & Hörber JKH, Academic Press. p.67-90
17. Charras GT & Horton MA. (2002) Determination of Cellular Strains by Combined Atomic Force Microscopy and Finite Element Modeling. Biophys J, 83, 2, P858-879.
18. Liu Y, Mollaeian K, Ren J et al. (2020) Effect of F-actin and microtubules on cellular mechanical behavior studied using atomic force microscope and an image recognition-based cytoskeleton quantification approach. Int J Mol Sci, 21:392.
19. Ogneva I, Levedev DV, Shenkman BS. (2010) Transversal stiffness and Young's modulus of single fibers from rat soleus muscle probed by atomic force microscopy. Biophys J 98:418-24.
20. Pastrana HF, Cartagena-Rivera AX, Raman A et al. (2019) Evaluation of the elastic Young's modulus and cytotoxicity variations in fibroblasts exposed to carbon-based nanomaterials. J Nanobiotechnol 17, 32. DOI 10.1186/s12951-019-0460-8
21. Nikolaev N, Muller T, Liu Y et al. (2014) Changes in the stiffness of human mesenchymal stem cells with the progress of cell death as measured by atomic force microscopy. J Biomech, 47:625-30.
22. Sokolov I, Lyer S, Venkatesh SR et. al. (2007) Detection of surface brush on biological cells in vitro with atomic force microscopy. Appl. Phys. Lett. 91, 023902. DOI: 10.1063/1.2757104

Corresponding author:

Ahmad A. Almazloum
Department of Electronics and Biomedical Engineering (DEEB),
School of Electrical and Computer Engineering (FEEC)
Av. Albert Einstein 400, Cidade Universitária Zeferino Vaz
Campinas – SP, 13083-852, Brazil
Email: ahmad@ceb.unicamp,br